Published in
Nuclear Instruments and Methods in Physics Research Section A:
Accelerators, Spectrometers, Detectors and Associated Equipment 560, issue 1, 122-126, 2006
which should be used for any reference to this work

TFA pixel sensor technology for vertex detectors

P. Jarron[a,*], D. Moraes[a,*], M. Despeisse[a], G. Dissertori[b], S. Dunand[c], J. Kaplon[a], C. Miazza[c], A. Shah[c], G.M. Viertel[b], N. Wyrsch[c]

[a]*CERN, CH-1211 Geneva 23, Switzerland*
[b]*ETH-Zurich, CH-8093 Zurich, Switzerland*
[c]*IMT, Rue A.-L. Breguet 2, CH-2000 Neuchatel, Switzerland*

Abstract

Pixel microvertex detectors at the SLHC and a future linear collider face very challenging issues: extreme radiation hardness, cooling design, interconnections density and fabrication cost. As an alternative approach we present a novel pixel detector based on the deposition of a Hydrogenated Amorphous Silicon (a-Si:H) film on top of a readout ASIC. The Thin-Film on ASIC (TFA) technology is inspired by an emerging microelectronic technology envisaged for visible light Active Pixel Sensor (APS) devices. We present results obtained with a-Si:H sensor films deposited on a glass substrate and on ASIC, including the radiation hardness of this material up to a fluence of 3.5×10^{15} p/cm^2.

Keywords: Hydrogenated amorphous silicon; TFA; Pixel detector; Radiation hardness

1. Introduction

A novel solid state detector technology based on the deposition of an Hydrogenated Amorphous Silicon (a-Si:H) film on top of an ASIC has been investigated. This technique provides sensor segmentation with a pixel size ranging from 25 to 500 μm at low cost and a supposed higher level of radiation hardness compared to crystal line silicon [1]. The vertical integration of a thin-film sensor on ASIC eliminates the need of bonding and enables a level of integration comparable to monolithic pixels while having the advantages of the hybrid pixel approach.

The a-Si:H characteristics were first studied on test devices, in which n–i–p diodes were evaporated on chromium-coated glass. These structures were characterised by measuring current versus voltage in the dark and under illumination, and transient charge collection efficiency [2].

After the optimisation of n–i–p diodes on glass substrates, these structures were deposited on ASICs. Some studies of charge collection efficiency under very weak pulsed light illumination and with beta sources for two different integrated circuits have been presented in Refs. [3,4].

2. Hydrogenated amorphous silicon

Amorphous Silicon (a:Si) is a semiconductor in which the silicon atoms are not arranged in the periodic lattice structure as in crystalline silicon. The relative position of atoms in a crystal is regularly ordered over large distances, while the amorphous structure has short-range order but lacks the long-range order. This disordered structure results in coordination defects such as dangling bonds and distorted Si–Si bonds in both lengths and angles, which induces energy levels in the forbidden energy gap where electrons and holes recombine. When amorphous silicon is hydrogenated (e.g. deposited by decomposition of SiH_4), the hydrogen atoms saturate the dangling bonds which act as recombination centres.

Hydrogenated amorphous silicon has much lower electron and hole mobilities than crystalline silicon, but it has the advantage of being produced at low cost in large-area depositions. In addition, it has the useful property of

*Corresponding authors. Tel.: +41 22 767 3842; fax: +41 22 767 3394.
E-mail addresses: Pierre.Jarron@cern.ch (P. Jarron), Danielle.Moraes@cern.ch (D. Moraes).

being deposited at low temperature (below 220 °C) and it has been proven to be a radiation hard material [1].

Its useful electrical properties were first reported by Spear and Le Comber [5] in 1976. Since then there has been considerable research and development of this material leading to a variety of applications such as photovoltaic panels, thin film light emitting diodes, photosensors and thin film transistors [6–10].

3. Irradiation of test structures

We first studied the characteristics of a-Si:H with test devices consisting of n–i–p diodes evaporated on chromium coated glass. The pixel areas were defined by a patterned Zinc Oxide (ZnO) or Indium Tin Oxide (ITO) top electrode. The patterning was achieved by a rubber stamping process followed by a wet etch of the transparent conductive oxide.

A test structure with 30 μm thick n–i–p a-Si:H diodes was used for irradiation tests. The diodes were squares of 4 mm^2 area, and were constantly reverse biased at 300 V. The test was performed at the CERN irradiation facility, which has a beam line of 24 GeV protons delivering a fluence up to 3×10^{13} protons/h cm^2.

The dose accumulated during the irradiation was 3.5×10^{15} protons/cm^2 over 4.8 days. Fig. 1 shows the current versus the number of spills obtained during irradiation. The "in beam" and "between beam" current is the current induced by the protons and the dark current, respectively. For reference the accumulated dose is indicated along the x-axis as dose markers, corresponding to 5.9×10^{13}, 1.55×10^{15} and 3.5×10^{15} protons/cm^2, from the left to the right. The dark current remains almost unchanged at about 200 nA up to the maximum measured fluence of 3.5×10^{15} protons/cm^2.

A dose of 1.5×10^{15} protons/cm^2 reduces the "in beam" current from about 8 μA down to approximately 4 μA. For higher doses it stabilizes around 2 μA. The current reduction is caused by metastable defects that affect both charge collection and depletion layer. The drop in the current is possibly due to the creation of radiation induced dangling bonds. Since the dangling bonds work as recombination centres for electron hole pairs this reduces the radiation-induced current in the detector. The stabilization can be explained by a thermal annealing effect that compensates radiation induced dangling bonds.

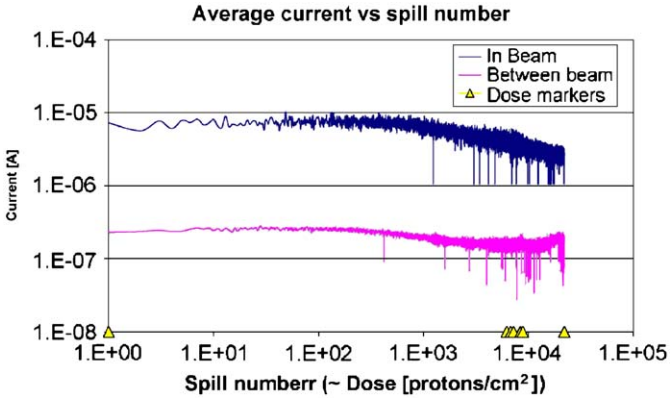

Fig. 1. Measured current as a function of the increasing radiation dose on a 30 μm n–i–p diode. The top curve shows the proton induced current and the bottom the total leakage current.

4. Macropixel sensor

The Macropixel sensor, shown in Fig. 2, consists of a film of a-Si:H deposited directly on top of an integrated circuit. The circuit is designed to study the characteristics of a-Si:H sensor. The sensor consists of a 15 μm thick a-Si:H film forming a n–i–p diode. The a-Si:H is deposited using the Very High Frequency Plasma Enhanced Chemical Vapour Deposition (VHF PCVD) process, which is crucial for achieving high deposition rates with minimal mechanical stress and low defect density [2]. The deposition is performed at a rate of 15.6 Å/s and a frequency of 70 MHz, using hydrogen dilution of Silane. The relatively low temperature of this process (between 180 and 220 °C) is compatible with post processing on finished electronic wafers.

The a-Si:H film consists of three layers: a top p-doped layer, an intrinsic sensitive layer and a bottom n-doped layer. The bottom layer is a thin (~20 nm) low-conductive layer that provides pixel isolation and avoids additional patterning of the ASIC. An ITO electrode, deposited by sputtering at room temperature, is used as top contact.

4.1. Integrated circuit

The integrated circuit is a 4×4 mm^2 ASIC implemented in 0.25 μm CMOS technology, powered with −2.5 V. It consists of 48 octagonal pads with about 140 μm width and 380 μm pitch, as shown in Fig. 2. Each pad is connected to a charge amplifier with active feedback followed by a stage providing CR–RC shaping. This architecture enables very high equivalent parallel noise resistance of the amplifier, which is crucial for optimisation of the noise performance.

The charge sensitive amplifier has a decay time constant that produces a slight undershoot of the output signals. This undershoot does not influence the noise performance of the circuit. The nominal value of the bias current of the

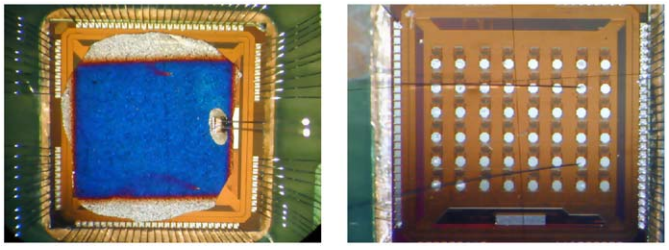

Fig. 2. Photograph of a Macropixel sensor (left) and integrated circuit (right). The sensor consists of an a-Si:H film deposited on top of the ASIC.

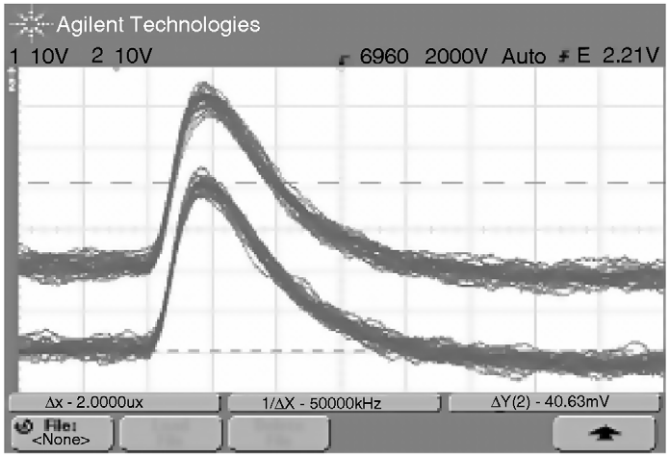

Fig. 3. Response of two randomly selected channels (not loaded) of the Macropixel ASIC to a 0.1 fC charge injected through a test capacitor. The horizontal and vertical scales show 200 ns and 10 mV per division, respectively. The bias current of the input transistor is set to 300 μA and the feedback current to 100 pA.

input transistor ranges between 200 and 400 μA. The amplifier is optimised to work with a feedback current of 100 pA and a detector leakage current of 10 pA. For leakage currents above the nominal value the bias of the feedback transistor can be increased up to 1 nA, with the penalty of increasing the parallel noise and the signal undershoot.

The shaper comprises two cascaded stages of amplifiers working in common source configuration based on PMOS and NMOS devices. The stages integrate signals with 100 ns time constant. An additional low-pass filter provides attenuation of high frequency components, which are not efficiently filtered by the main shaper stage, without influencing the pulse gain of the full chain. The circuit functionality can be tested by injecting calibration pulses via a 5 fF internal capacitor connected to each channel input.

The Macropixel circuit has a measured gain of 430 mV/fC and a peaking time of about 160 ns. The measured equivalent noise charge is between $20e^-$ and $27e^-$ for the feedback current varying from 30 to 220 pA. Fig. 3 shows the response of two randomly selected channels (not loaded) to a 0.1 fC ($625e^-$) charge injected through a test capacitor. Although the circuit has been optimised for negative input charges it can work with positive signals in a limited dynamic range.

5. Sensor performance

A negative bias voltage is applied to the top contact (ITO layer) of the Macropixel sensor, depleting the n–i–p diode and increasing the depleted layer from the p–i interface down towards the i–n interface. The charge deposited is drifted by the electric field in the depleted layer inducing a signal on the pads connected to the amplifier. Fig. 4 shows a cross-section of the sensor.

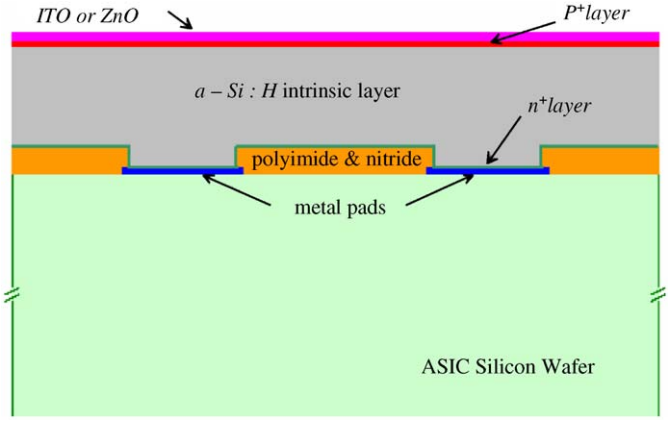

Fig. 4. Cross-section of the Macropixel sensor.

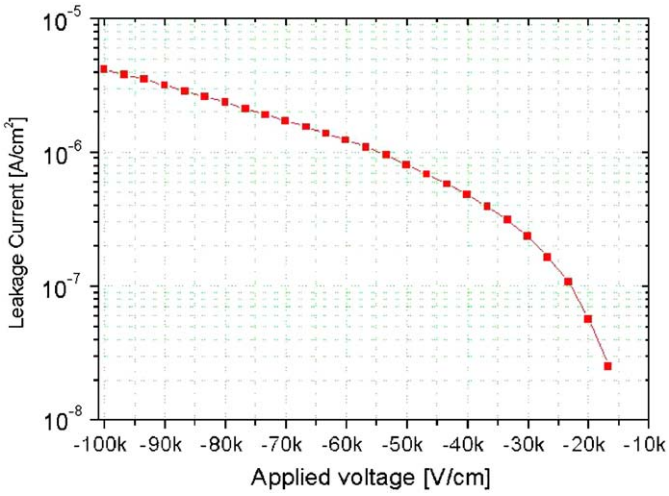

Fig. 5. Measured leakage current of the 48 sensor pixels as a function of the applied voltage across the sensor thickness.

5.1. Dark current

Fig. 5 shows the sensor leakage current measured as a function of the applied voltage across the sensor thickness. The leakage current is directly measured from the biasing circuit. For an applied voltage of about 10^5 V/cm the leakage current is measured to be 700 pA. This value is larger than the expected values from test samples and is mainly due to the non-flatness of the ASIC surface, caused by the passivation and metal layers.

The leakage current is field dependent and the non-flatness of the substrate induces high field regions at the pixel edges, thereby increasing the leakage current.

5.2. Noise measurement

Fig. 6 shows the noise distribution at a reverse bias of 145 V and a feedback current of 800 pA. A feedback current larger than the nominal value had to be applied to compensate the increase of the sensor leakage current. An

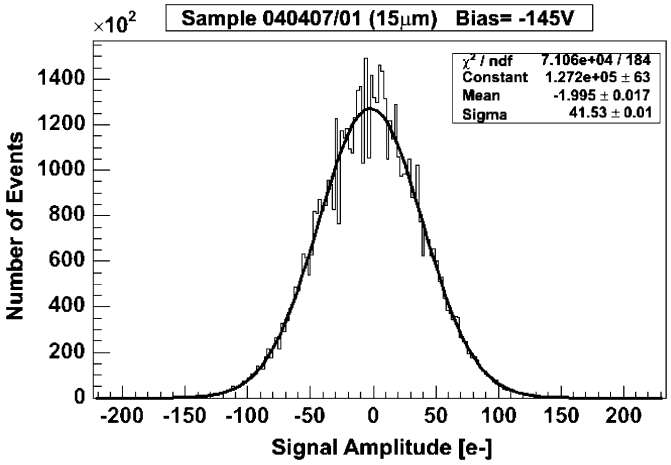

Fig. 6. Equivalent noise charge measured for the Macropixel sensor with a reverse bias of 145 V and a feedback current equal to 800 pA.

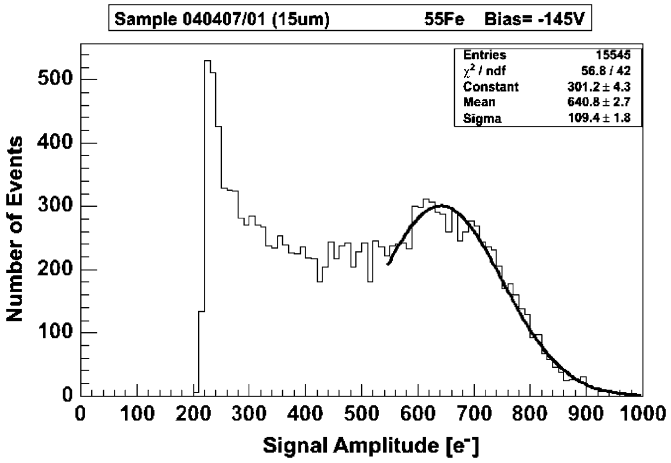

Fig. 7. Spectrum of 5.9 keV photons from a ^{55}Fe source on the Macropixel sensor, with a reverse bias voltage equal to 145 V and a threshold of 200e$^-$.

equivalent noise charge of 41.5e$^-$ r.m.s. was measured. This measurement was performed using a digital oscilloscope. The noise is in good agreement with calculations.

5.3. Particle detection

Detection of particles is achieved in self-trigger mode with a radioactive source placed directly on top of the sensor at a distance of approximately 5 mm. The trigger level was set at about five sigma above the noise level. The signal from the sensor was read out by an oscilloscope/LabView system to measure and to store the signal pedestals and amplitudes.

Fig. 7 shows the spectrum obtained with a 5.9 keV energy ^{55}Fe source, at a reverse bias voltage of 145 V. A peak at about 640e$^-$ was measured. For crystalline silicon the expected signal from this source would be about 1600e$^-$. Assuming that the pair creation energy for a-Si:H is approximately 4 eV and that only a maximum of 30% of the holes produced are collected at 160 ns, due to their low mobility, a signal of 958e$^-$ would be expected. This simple calculation suggests that the collected charge is not complete, either because the diode is not fully depleted or because of possible loss of signal due to charge recombination. Fig. 8 shows the measured peak amplitude for the ^{55}Fe source as a function of the applied voltage across the sensor thickness.

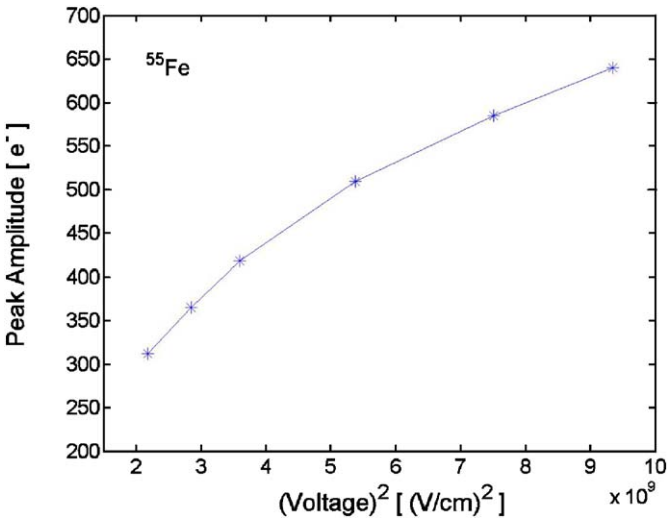

Fig. 8. Peak amplitude from a ^{55}Fe source as a function of the applied voltage to the Macropixel sensor.

6. Conclusion

A Macropixel sensor based on the deposition of a 15 μm a-Si:H film on top of the ASIC has been developed. The deposition was performed via VHF PCVD. The sensor shows a very low noise of about 41e$^-$. Measurements with photons from an iron source (^{55}Fe) showed that there is incomplete charge collection at an applied voltage of 10^5 V/cm.

A test device, 30 μm thick and evaporated on chromium coated glass, was used for irradiation tests. The a-Si:H film was irradiated over 4.8 days with a total accumulated dose of 3×10^{15} protons/cm^2. The irradiated device shows a reduction in the current induced by charged particles, without a significant increase of the leakage current. In our test we have used dose rates of about 10^{11}–10^{12} protons/cm^2 s which are four orders of magnitude higher than in LHC.

Electrical properties of hydrogenated amorphous silicon materials are being investigated. So far it has been observed a strong-annealing effect has been observed, indicating that a-Si:H sensors can sustain a very high fluence up to 10^{16} protons/cm^2 to the extent that annealing of metastable defects is complete or the dose rate exposure is sufficiently low, as is the case in the LHC.

Initial studies of a-Si:H pixel sensors seem very promising but further developments are required to understand the charge collection and radiation hardness of thick a-Si:H films.

Acknowledgments

The authors would like to express thanks to Maurice Glaser and Federico Ravotti for their important help and contributions to the radiation tests.

References

[1] N. Kishimoto, H. Amekura, K. Kono, C.G. Lee, J. Nucl. Mater. 258–263 (1998) 1908;
N. Kishimoto, H. Amekura, K. Kono, C.G. Lee, J. Non-Cryst. Solids 227–230 (1998) 238.

[2] N. Wyrsch, S. Dunand, C. Miazza, A. Shah, G. Anelli, M. Despeisse, A. Garrigos, P. Jarron, J. Kaplon, D. Moraes, S.C. Commichau, G. Dissertori, G.M. Viertel, Phys. Stat. Sol. C 1 (2004) 1284.

[3] D. Moraes, G. Anelli, M. Despeisse, G. Dissertori, A. Garrigos, P. Jarron, J. Kaplon, C. Miazza, A. Shah, G.M. Viertel, N. Wyrsch, J. Non-Cryst. Solids 338–340 (2004) 729.

[4] P. Jarron, G. Anelli, S.C. Commichau, M. Despeisse, G. Dissertori, C. Miazza, D. Moraes, A. Shah, G.M. Viertel, N. Wyrsch, Nucl. Instr. and Meth. A 518 (2004) 366 and Nucl. Instr. and Meth. A 518 (2004) 357.

[5] W.E. Spear, P.G. Le Comber, Philos. Mag. 33 (1976) 935.

[6] R.A. Street, Hydrogenated Amorphous Silicon, Cambridge University Press, Cambridge, 1991, ISBN:0521371562.

[7] J. Kanichi, Amorphous and Microcrystalline Semiconductors Devices: Optoelectronic Devices, Artech House, 1991, ISBN:0-89006-490-3.

[8] V.′ Perez-Mendez, G. Cho, J. Drewery, T. Jing, S.N. Kaplan, S. Qureshi, D. Wildermuth, I. Fujieda, R.A. Street, J. Non-Cryst. Solids 137 (1991) 1291.

[9] R.A. Street, X.D. Wu, R. Weisfield, S. Ready, R. Apte, M. Nguyen, P. Nylen, in: Proceedings of the Ninth Workshop on Room-Temperature Semiconductors, X- and γ-ray Detectors, Grenoble, 18–22 September 1995.

[10] J.L. Crowley, Solid State Technol. (1992) 94.